

A GNSS-R FORWARD MODEL FOR DELAY-DOPPLER MAP ASSIMILATION

Feixiong Huang¹, James L. Garrison¹, Mark Leidner², Bachir Annane³, Ross Hoffman²

¹Purdue University, West Lafayette, USA

²Atmospheric and Environmental Research, Lexington, MA, USA

³Cooperative Institute for Marine and Atmospheric Studies (CIMAS), Miami, FL, USA

ABSTRACT

The Cyclone Global Navigation Satellite System (CYGNSS) constellation was launched for the purpose of improving tropical cyclone forecasts using GNSS Reflectometry (GNSS-R). CYGNSS wind speed estimates have been based on only a small window of the Delay-Doppler Maps (DDM) due to the resolution requirement. Direct assimilation of DDM data into a forecast model is an alternative approach, that could take advantage of contribution to the DDM from regions on the ocean away from the specular point. This paper will present a generalized forward model for assimilation of DDMs into a weather model. The forward operator and Jacobian matrix are derived and structured for use in data assimilation systems. The model has also been assessed using CYGNSS Level 1 data from the 2017 Hurricane season.

Index Terms— GPS, GNSS-R, DDM, data assimilation, ocean wind, VAM

1. INTRODUCTION

The Delay-Doppler Map (DDM) is produced from cross-correlation between the local GPS baseband signal and the scattering power from the ocean surface (glistening zone) over a range of delays and Doppler frequencies [1]. The CYGNSS Level 1 product includes a calibrated 17×11 DDM around the specular point with 17 delay bins (resolution of 0.25 chips) and 11 Doppler bins (resolution of 500 Hz) [2]. Wind speed retrieval is a CYGNSS Level 2 product. Limited by the 25 km spatial resolution requirement, the baseline wind speed retrieval uses observables only from the 3×5 DDM aligned with the specular point [3], [4]. One major application of the CYGNSS products is to assimilate the data into numerical weather model to improve hurricane forecasts and there has been some research on assimilation of CYGNSS Level 2 wind speeds [5], [6].

However, the CYGNSS wind speeds are computed from only 8% of the pixels in the DDM, discarding a lot of potential information. The motivation of the research in the paper is to directly assimilate the calibrated full 17×11 DDMs

This work was supported by NASA Grant NNX15AU18G, Assimilation of GNSS-R Delay-Doppler Maps into Hurricane Models.

into a hurricane forecast model. The development of a forward model which links the wind field and the DDM is the prerequisite for data assimilation. A description of the forward model is presented in section 2, the use of the model in data assimilation is described in section 3, assessment of the model on real data is shown in section 4 and the conclusions are stated in section 5.

2. MODEL DESCRIPTION

The forward operator produces a DDM from a field of mean square slope (MSS), \mathbf{m} by a numerical surface integration of the bistatic radar equation [1].

$$h(\tau, f, \mathbf{m}) = \frac{\lambda^2 P_t}{(4\pi)^3} \sum_i \frac{G_t(\vec{\rho}_i) G_r(\vec{\rho}_i)}{R_t^2(\vec{\rho}_i) R_r^2(\vec{\rho}_i)} \times \chi^2(\Delta\tau(\vec{\rho}_i), \Delta f(\vec{\rho}_i)) \sigma^0(\vec{\rho}_i, m_i) dS_i \quad (1)$$

In the Kirchoff Approximation Geometric Optics model, the bistatic radar cross section (BRCS) is proportional to the probability density function of surface slopes $P(m, \vec{s})$.

$$\sigma^0 = \pi |\Re|^2 \frac{q^4}{q_z^4} P(m, \vec{s}) \quad (2)$$

For our applications, the surface slopes \vec{s} are assumed to have an isotropic normal distribution,

$$P(m, \vec{s}) = \frac{1}{2\pi m} \exp\left(-\frac{s^2}{2m}\right) \quad (3)$$

allowing an analytical expression for the Jacobian to be derived.

The Jacobian matrix is computed by linearizing the forward operator and then taking partial derivative respect to MSS, from Eq. (4).

$$\mathbf{H} = \begin{bmatrix} \frac{\partial h(\tau_1, f_1, \mathbf{m})}{\partial m_1} & \dots & \frac{\partial h(\tau_1, f_1, \mathbf{m})}{\partial m_M} \\ \vdots & \dots & \vdots \\ \frac{\partial h(\tau_1, f_N, \mathbf{m})}{\partial m_1} & \dots & \frac{\partial h(\tau_1, f_N, \mathbf{m})}{\partial m_M} \\ \frac{\partial h(\tau_2, f_N, \mathbf{m})}{\partial m_1} & \dots & \frac{\partial h(\tau_2, f_N, \mathbf{m})}{\partial m_M} \\ \vdots & \dots & \vdots \\ \frac{\partial h(\tau_N, f_N, \mathbf{m})}{\partial m_1} & \dots & \frac{\partial h(\tau_N, f_N, \mathbf{m})}{\partial m_M} \end{bmatrix} \quad (4)$$

In our implementation of the forward model, four input structures and two output structures are defined which are shown in Figure 1. The input structures are *metadata*, *powerParm*, *inputWindField* and *Geometry*, where *metadata* defines the parameters of the DDM bins, thermal noise and surface grid; *powerParm* stores power and antenna parameters of transmitter and receiver; *inputWindField* stores the wind field data where the MSS can be calculated from the wind speed by an empirical model (e.g. [7]); and *Geometry* stores the positions and velocities of transmitter and receiver. The output structures are *DDM* and *Jacobian*, which store the DDM power computed from the model and its corresponding Jacobian matrix.

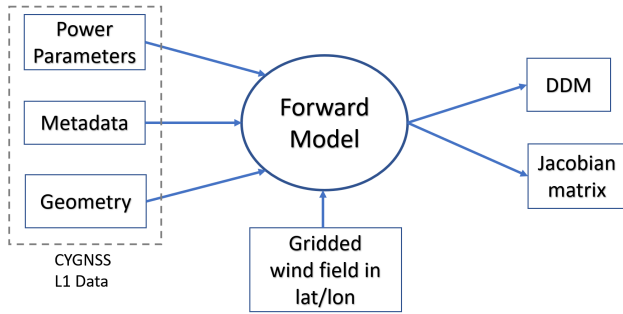


Fig. 1. Structure of Forward Model

In order to integrate the forward model into data assimilation system, this model is designed to be a single callable function in C/C++ language with all inputs and outputs stored in memory that can be merged into data assimilation code. The Jacobian matrix is computed along with the simulated DDM. Significant code has been reused from the CYGNSS End-to-End Simulator (E2ES) [8].

3. DATA ASSIMILATION METHOD

The approach used to assimilate DDMs is the Variational Analysis Method (VAM) which integrates DDMs into a two-dimensional wind vector field [9]. Starting with an a priori gridded wind vector field (background), the VAM produces gridded VAM-CYGNSS vector winds (analysis) by minimizing a cost function J [10].

$$J(\mathbf{x}) = J_b(\mathbf{x}) + J_o(\mathbf{x}) + J_c(\mathbf{x}) \quad (5)$$

where \mathbf{x} is the analysis wind field, $J_b(\mathbf{x})$, $J_o(\mathbf{x})$ are normalized misfits of the analysis to the background and observations, $J_c(\mathbf{x})$ is the dynamic constraints.

To start the minimization, the VAM analysis winds are first set equal to the background winds. Then the increment in MSS is computed as:

$$\Delta \mathbf{m} = \frac{\mathbf{B}\mathbf{H}^T}{\mathbf{H}\mathbf{B}\mathbf{H}^T + \mathbf{R}}(\mathbf{y} - \mathbf{h}(\mathbf{m}_a)) \quad (6)$$

where \mathbf{m}_a is MSS field of the analysis, \mathbf{y} is the measured DDM, $\mathbf{h}(\cdot)$ is the forward operator. \mathbf{B} , \mathbf{R} are estimated covariance matrices of the background and observation error, respectively. The increment of MSS, $\Delta \mathbf{m}$, is transformed into increment of wind speed magnitude by an empirical model (e.g. [7]). The increment of wind speed magnitude is then applied to the analysis winds without changing the wind direction and the cost function J will be updated. The VAM's solution is found by iteratively minimizing J until convergence criteria are met.

4. FORWARD MODEL ASSESSMENT

To test the forward model, CYGNSS L1 data from hurricane Irma on September 4, 2017 was processed. The track of CYGNSS passed over the hurricane around 23:40 UTC. Wind field data for comparison were obtained from the Hurricane Weather Research and Forecasting (HWRF) forecast model for 23:00 UTC. Figure 2 shows the CYGNSS satellite track and the HWRF 5-h forecast wind field.

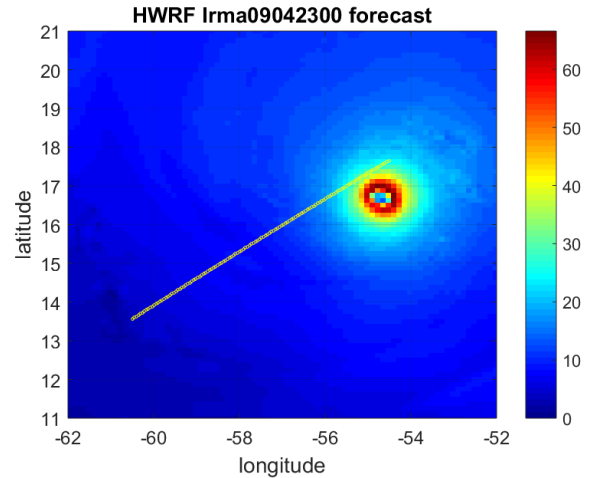


Fig. 2. CYGNSS track and HWRF wind field

Two specular points were chosen for comparison between the observed CYGNSS DDM and the forward model computed DDM. The first is near the hurricane where surface wind speeds are high and variable. The other is far from the eye where winds are low and homogeneous. The positions and velocities of transmitter and receiver, all power parameters from CYGNSS L1 data and wind field from HWRF were read by the forward model. Figure 3 and 4 show good comparison between CYGNSS DDMs and forward model DDMs. They both show good match-up including the asymmetries in the pattern.

Statistics were computed for comparison over a track of 120 DDMs. For each pair of DDMs from observation and forward model, the average relative power difference of ef-

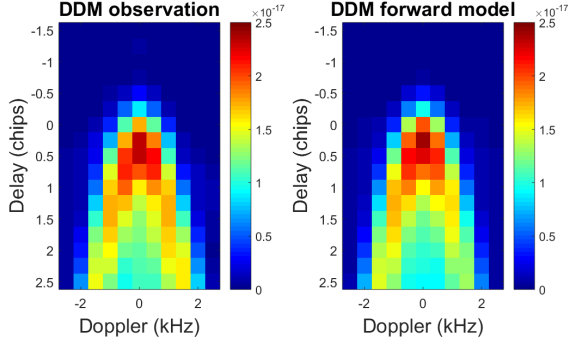


Fig. 3. DDM comparison near hurricane

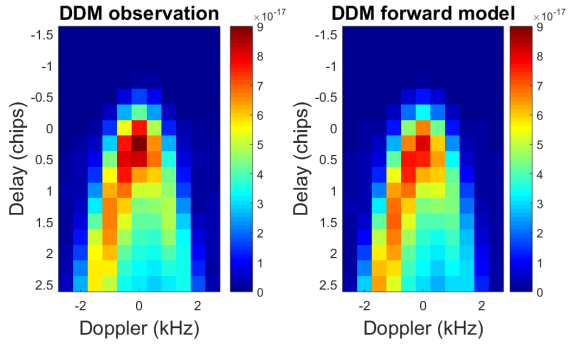


Fig. 4. DDM comparison at low wind speed

ffective bins is computed.

$$\epsilon_k = \frac{1}{N} \sum_{i,j} \frac{y_k(\tau_i, f_j) - h_k(\tau_i, f_j)}{y_k(\tau_i, f_j)} \quad (7)$$

where k is the sample index, $y(\tau, f)$ is the observed DDM, $h(\tau, f)$ is the forward model DDM, (i, j) is the delay/Doppler indices of effective bins, N is the number of effective bins and ϵ is the relative difference.

Figure 5 shows that the relative differences of this track are all below 40%. The differences between observed ones and simulated ones are likely caused by an inaccurate transmitter power, the presence of swell and limitations of the scattering model.

Since an inaccurate transmitter power could result in a proportional power error, an excess power is added as control variable into the forward model. For the track of DDMs in this test, each forward model DDM is then added by an excess power by fitting them with the observed DDM using the least squares method. Figure 6 shows the relative difference after adding the excess power and Figure 7 shows the excess power of the track in unit of dB. The average excess power of the track is 1.37 dB and the comparison becomes much better with the excess power.

The Jacobian matrix was validated by comparison with finite differences. The forward model computes Jacobian matrix by an analytical form which is very efficient (taking about

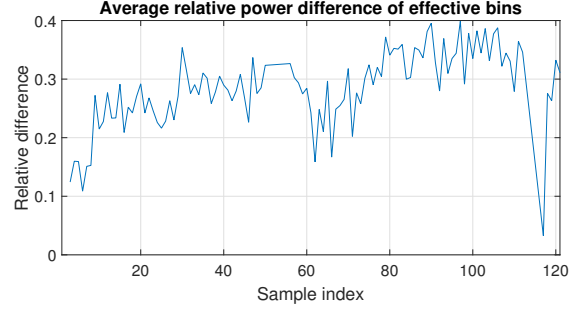


Fig. 5. Relative differences of a track of DDMs

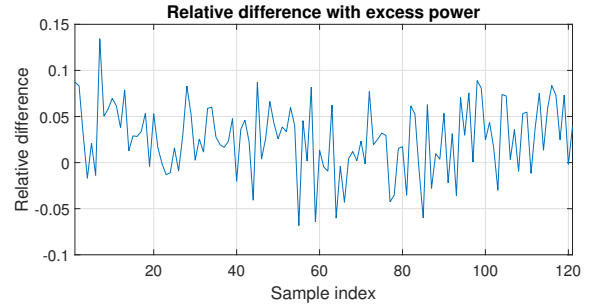


Fig. 6. Relative differences with excess power

1s). The matrix could also be computed by finite difference which could be more robust but inefficient (taking about 30s-40s). Figure 8 shows the Jacobian matrices computed by analytical form and finite difference. It can be seen that they have the similar patterns and values. The relative error is about 6% in average and the correlation coefficient between the two matrices is 0.9991. Thus the model Jacobian matrix is expected to be a good representation of the sensitivity of wind field at a low computational cost.

5. CONCLUSION

A forward model has been developed for direct assimilation of DDM into hurricane models. This model takes in

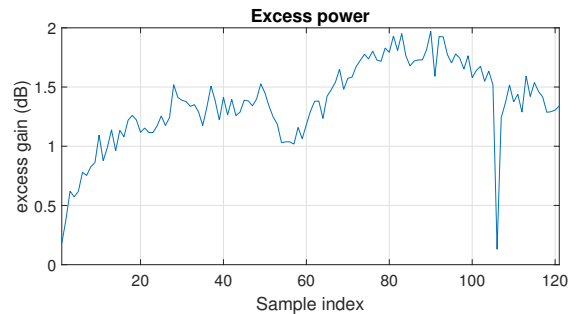


Fig. 7. Excess power in unit of dB

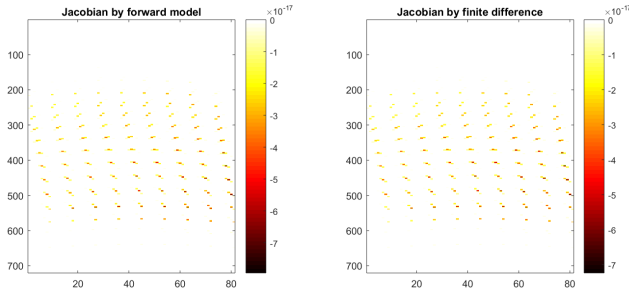


Fig. 8. Computation of Jacobian matrix by analytical form and finite difference

CYGNSS level 1 data and outputs a DDM with a partial derivative matrix. These are designed for use in the VAM to assimilate CYGNSS measured DDMs and update a wind vector field. The model has been tested against CYGNSS DDM measurements collected around Hurricane Irma. Simulated DDMs calculated by the forward operator show qualitative agreement with CYGNSS measured DDMs. An excess power variable is added to the forward model to offset the error in transmitter power calibration. The Jacobian matrix is validated by comparison with finite difference estimates. Future work could include incorporating data from the wave field to improve its performance in low wind speed cases and including additional variables to account for instrument effects, such as delay-Doppler offsets.

6. REFERENCES

- [1] Valery U Zavorotny and Alexander G Voronovich, "Scattering of GPS signals from the ocean with wind remote sensing application," *IEEE Transactions on Geoscience and Remote Sensing*, vol. 38, no. 2, pp. 951–964, 2000.
- [2] Scott Gleason, Christopher S Ruf, Maria Paola Clarizia, and Andrew J O'Brien, "Calibration and unwrapping of the normalized scattering cross section for the Cyclone Global Navigation Satellite System," *IEEE Transactions on Geoscience and Remote Sensing*, vol. 54, no. 5, pp. 2495–2509, 2016.
- [3] Maria Paola Clarizia, Christopher S Ruf, Philip Jales, and Christine Gommenginger, "Spaceborne GNSS-R minimum variance wind speed estimator," *IEEE transactions on geoscience and remote sensing*, vol. 52, no. 11, pp. 6829–6843, 2014.
- [4] Maria Paola Clarizia and Christopher S Ruf, "Wind speed retrieval algorithm for the Cyclone Global Navigation Satellite System (CYGNSS) mission," *IEEE Transactions on Geoscience and Remote Sensing*, vol. 54, no. 8, pp. 4419–4432, 2016.
- [5] Shixuan Zhang, Zhaoxia Pu, Derek J Posselt, and Robert Atlas, "Impact of CYGNSS ocean surface wind speeds on numerical simulations of a hurricane in observing system simulation experiments," *Journal of Atmospheric and Oceanic Technology*, vol. 34, no. 2, pp. 375–383, 2017.
- [6] Brian McNoldy, Bachir Annane, Sharanya Majumdar, Javier Delgado, Lisa Bucci, and Robert Atlas, "Impact of assimilating CYGNSS data on tropical cyclone analyses and forecasts in a regional OSSE framework," *Marine Technology Society Journal*, vol. 51, no. 1, pp. 7–15, 2017.
- [7] Stephen J Katzberg, Omar Torres, and George Ganoë, "Calibration of reflected GPS for tropical storm wind speed retrievals," *Geophysical Research Letters*, vol. 33, no. 18, 2006.
- [8] A OBrien, "CYGNSS end-to-end simulator," *CYGNSS Project Doc*, pp. 148–0123, 2014.
- [9] Robert Atlas, Ross N Hoffman, Joseph Ardizzone, S Mark Leidner, Juan Carlos Jusem, Deborah K Smith, and Daniel Gombos, "A cross-calibrated, multiplatform ocean surface wind velocity product for meteorological and oceanographic applications," *Bulletin of the American Meteorological Society*, vol. 92, no. 2, pp. 157–174, 2011.
- [10] RN Hoffman, SM Leidner, JM Henderson, R Atlas, JV Ardizzone, and SC Bloom, "A two-dimensional variational analysis method for NSCAT ambiguity removal: Methodology, sensitivity, and tuning," *Journal of Atmospheric and Oceanic Technology*, vol. 20, no. 5, pp. 585–605, 2003.